Research article

Identifying autophagy-related mRNAs and potential ceRNA networks in meniscus degeneration based on RNA sequencing and experimental validation

Jun Zhang [a,b,1], Jiayong Zhu [b,1], Xinyu Zou [b,1], Yiming Liu [b], Boming Zhao [b], Liaobin Chen [b,**], Bin Li [b,***], Biao Chen [b,*]

[a] *Department of Orthopedics, The First Hospital of Nanchang, The Third Affiliated Hospital of Nanchang University, Nanchang, 330008, Jiangxi, China*
[b] *Division of Joint Surgery and Sports Medicine, Department of Orthopedic Surgery, Zhongnan Hospital of Wuhan University, Wuhan, 430000, Hubei, China*

ARTICLE INFO

ABSTRACT

Purpose: The intimate connection between long noncoding RNA (lncRNA) and autophagy has been established in cartilage degeneration. However, their roles in meniscal degeneration remain ambiguous. This study aimed to identify the key autophagy-related lncRNA and its associated regulatory network in meniscal degeneration in the context of osteoarthritis (OA).

Methods: RNA sequencing was performed to identify differentially expressed lncRNAs (DELs) and mRNAs (DEMs), which were then conducted to enrichment analyses using the DAVID database and Metascape. Autophagy-related DEMs were identified by combining DEMs with data from the Human Autophagy Database. Three databases were used to predict miRNA, and the DIANA LncBase Predicted database was utilized to predict miRNA-lncRNA interactions. Based on these predictions, comprehensive competitive endogenous RNA (ceRNA) network were constructed. The expression levels of the classical autophagy markers and autophagy-related ceRNA network were validated. Additionally, Gene Set Enrichment Analysis (GSEA) was performed using autophagy-related DEMs.

Results: 310 DELs and 320 DEMs were identified, with five upregulated and one downregulated autophagy-related DEMs. Through reverse prediction of miRNA, paired miRNA-lncRNA interactions, and verification using RT-qPCR, two lncRNAs (PCAT19, CLIP1-AS1), two miRNA (has-miR-3680-3p and has-miR-4795-3p) and two mRNAs (BAG3 and HSP90AB1) were included in the constructed ceRNA regulatory networks. GSEA indicated that the increased expression of autophagy-related mRNAs inhibited glycosaminoglycan biosynthesis in the degenerative meniscus.

Conclusion: This study presented the first construction of regulatory ceRNA network involving autophagy-related lncRNA-miRNA-mRNA interactions in OA meniscus. These findings offered

valuable insights into the mechanisms underlying meniscal degeneration and provided potential targets for therapeutic intervention.

1. Introduction

The menisci serve as vital tissues for the proper functioning of the knee joint, playing a critical role in load transmission, stability, and shock absorption [1]. With advancing age, the macro- and micro-architecture of the meniscus undergo degenerative changes, resulting in meniscal damage and subsequent development of osteoarthritis (OA) [2]. The prevalence of meniscal degeneration rises with age, affecting approximately 50 % of individuals aged 70 and above. These degenerative lesions, combined with cartilage degeneration, contribute to knee joint pain and dysfunction [3]. Moreover, middle-aged patients (>40 years) face an increased risk of degenerative meniscal tears, which significantly impede daily activities and diminish quality of life. Consequently, it is imperative to gain a deeper understanding of the molecular mechanisms underlying meniscal degeneration in the presence of OA.

Autophagy, known as a non-selective catabolic pathway [4], has been implicated in various disease processes such as infectious diseases, cancer, neurodegenerative disorders, aging, and cardiovascular diseases [5]. Previous studies have focused on autophagy-related changes and their implications in the cartilage degeneration of OA and intervertebral disc [6,7]. Notably, a recent study reported a significant increase in the expression level of the autophagy-related protein ATG5 in meniscal tissue, both within and adjacent to the injury site, in a mouse model of destabilizing the medial meniscus-induced OA (DMM-OA), while ATG-5 expression was reduced in the posterior region [8]. Therefore, the precise role and underlying molecular mechanisms of autophagy in meniscal degeneration in human OA remain poorly understood.

Long non-coding RNA (lncRNA) refers to RNA transcripts that exceed 200 nucleotides in length. These transcripts have been found to regulate mRNA expression by acting as competitive endogenous RNA (ceRNA), effectively sequestering microRNAs (miRNAs) and thereby playing crucial roles in cell growth, response to various pressures and stimuli, and the proper functioning of the nervous, muscle, cardiovascular, hematopoietic, and immune systems [9,10]. Previous studies have shown that lncRNAs could regulate cartilage development, degeneration and regeneration [11]. For instance, lncRNA PACER, located upstream of COX-2, governed the expression levels of COX-2, thereby promoting cartilage degeneration in osteoarthritis [12,13]. Acting as a miR-25-3p sponge, lncRNA OIP5-AS1 contributed to intervertebral disc degeneration by degrading critical components of the extracellular matrix, such as collagen type II and aggrecan [14]. Furthermore, recent studies have highlighted the role of lncRNAs in the regulation of cartilage aging and degeneration through their interactions with autophagy-related genes. LncRNA cIR modulated the expression levels of autophagy-related proteins (LC3BI/II and Beclin 1), leading to the degradation of the extracellular collagen matrix and the worsening of articular cartilage degeneration [15]. By promoting the autophagy and apoptosis of nucleus pulposus cells through the miR-139/CXCR4/NF-κB axis, lncRNA h19 intensified the degree of intervertebral disc degeneration [16]. Nevertheless, there remains a dearth of research investigating the mechanisms and roles of autophagy-related lncRNAs in meniscal degeneration.

In order to gain deeper insights into the role of autophagy-related lncRNAs and their regulatory network in meniscal degeneration associated with OA, we conducted RNA sequencing analysis on both OA meniscus and non-OA meniscus samples. Using bioinformatics methodologies, we identified a set of differentially expressed lncRNAs (DELs) and mRNAs (DEMs) specifically in the OA meniscus, with a specific focus on autophagy-related DEMs. Subsequently, we constructed a comprehensive autophagy-related lncRNA-miRNA-mRNA network. To ensure the reliability of the identified autophagy-related DELs and DEMs from the RNA sequencing data, we conducted a validation study employing Real-Time Quantitative Polymerase Chain Reaction (RT-qPCR). Lastly, we performed Gene Set Enrichment Analysis (GSEA) to investigate the enrichment of autophagy-related mRNAs within the ceRNA network.

2. Materials and methods

2.1. Human meniscus tissues from normal and aging knees

The study was approved by the Ethics Committee of Zhongnan Hospital of Wuhan University (No. 2022069K), and all participating patients provided written informed consent. Detailed information regarding age, sex, and body mass index was recorded for each patient. Inclusion criteria for the non-OA meniscus group without osteoarthritis (OA) were as follows: (1) prior treatment with arthroscopic partial meniscectomy, and (2) absence of cartilage destruction or osteoarthritis. For the OA meniscus group, the inclusion criteria were: (1) presence of cartilage degeneration and bone degeneration, and (2) patients undergoing knee replacement surgery. Immediately after surgical excision, the meniscal tissue was transferred to RNAlater solution (Thermo Fisher Scientific), refrigerated overnight at 4 °C, and stored at −80 °C. Ten samples (including 5 samples older than 40 years with OA and 5 samples younger than 40 years without OA) were used to perform RNA sequencing, and other sixteen samples (including 8 samples older than 40 years with OA and 8 samples younger than 40 years without OA) were used for RT-qPCR.

3. RNA sequencing

Following the manufacturer's guidelines, total RNAs were extracted from meniscal tissue samples obtained from five cases and five controls, utilizing TRIzol (Invitrogen, cat. NO 15596026). The concentration and purity of the extracted total RNA samples were assessed using the Qubit3.0 system with the QubitTM RNA Broad Range Assay kit (Life Technologies, Q10210). For sequencing

purposes, the KCTM Stranded mRNA Library Prep Kit for Illumina® (Catalog NO. DR08402, Wuhan Seqhealth Co., Ltd. China) was employed as per the manufacturer's instructions. PCR products corresponding to 200–500 base pairs were enriched, quantified, and subsequently subjected to sequencing on the Novaseq 6000 sequencer (Illumina) using the PE150 model. Expression values for both lncRNAs and mRNAs were reported as reads per kilobase per million reads mapped (RPKM), following the method described by *Mortazavi* et al. [17]. In cases where multiple transcripts were associated with a single gene, the longest transcript was selected to calculate its abundance and coverage. Annotation was performed based on the human reference genome GRCh38. Detailed clinical parameters of RNA sequencing samples are summarized in Table S1.

4. Data processing

Initially, the RPKM values were transformed into log2 values and subjected to quantile normalization using the LIMMA package in R. To establish screening thresholds, the following criteria were employed: P value < 0.05 and the absolute log2 fold change ($|\log2(FC)|$) >0.5 for differentially expressed mRNAs (DEMs), while a P value of less than 0.05 and $|\log2(FC)|$ greater than 1 were utilized for differentially expressed lncRNAs (DELs). Volcano plots and heatmaps were generated using the GGplot2 package in R.

4.1. Enrichment analysis of DEMs

To further understand the biological function of DEMs, enrichment analyses based on Gene Ontology (GO) and Kyoto Encyclopedia of Genes and Genomes (KEGG) pathways were performed using the Database for Annotation, Visualization, and Integrated Discovery (DAVID) (version 6.8) [18]. GO, KEGG and Reactome pathway functional enrichment were also conducted based on the Metascape [19].

4.2. Identification of autophagy-related DEMs

222 autophagy-related genes were obtained from The Human Autophagy Database (http://www.autophagy.lu/index.html). By intersecting autophagy-related mRNAs with DEMs, we obtained a group of differentially expressed autophagy-related mRNAs (autophagy-related DEMs). To further understand the biological function of autophagy-related DEMs, enrichment analyses based on Gene Ontology (GO) and Kyoto Encyclopedia of Genes and Genomes (KEGG) pathways were performed using the KOBAS 3.0 [20].

4.3. Construction of a lncRNA-miRNA-mRNA network

First, the intersection of three databases, including Targetscan [21], miRmap [22] and miRDB [23] were used to predict miRNA of autophagy-related DEMs. It is worth noting that, we extracted the miRNAs targeting >2 mRNAs in the three databases as our prediction final results. Then, based on predicted miRNAs, potential lncRNA targeting miRNAs were predicted using the DIANA-LncBase Predicted database (version 2) [24] with thresholds of miTG-score >0.9, and intersected the results with DELs as the final hub lncRNAs. Finally, the lncRNA-miRNA-mRNA network was established and visualized by Cytoscape software (version 3.9.1).

4.4. Real-time Quantitative Polymerase Chain reaction (RT-qPCR)

Total RNAs were extracted from human meniscal tissues using Trizol Reagent according to the manufacturer's instructions. And

Table 1
Primer sequences for RT-qPCR.

Gene	Forward primer	Reverse primer
CLIP1-AS1	TGTAAGCAAAAGGTCAAGG	GTGATGCCGCTCTATGTG
PCAT19	ATGTTCACCCCAACCTCC	CCCCTAATTCGGCTCTTA
HSP90AB1	CTGGTGGTGCTGCTGTTT	TAGATGCGGTTGGAGTGG
ATG4A	CCCTTATCTGTAGACACTTGG	CACTGTAGGATGCGTTGG
BAG3	GCTCCAGTTCCTTGTCCT	CCTGGTTTTGGAGGTGTA
PEA15	ACCAACAACATCACCCTT	GTGAGTAGGTCAGGACGG
GAPDH	CTCAACAGGGATGCTTACCCC	GATACGGCCAAATCCGTTCA
MIR3680-3p	CGCGCGGCAGACCCGG	AGTGCAGGGTCCGAGGTATT
MIR4795-3p	GCGCGCGCGAAAAGCC	AGTGCAGGGTCCGAGGTATT
MIR4736	GCGCGCGAGGCAGGAC	AGTGCAGGGTCCGAGGTATT
U6	CTCGCTTCGGCAGCACA	AGTGCAGGGTCCGAGGTATT
LC3B	TCATCAAGATAATTAGAAGGCGCT	AACAATTCTAGAAGAGCTGCATTT
SQSTM1	CCATTGCGGAGCCTCATCTC	GTCCCCGTCCTCATCCTTTC
Beclin1	GGTTGCGGTTTTTCTGGGAC	CTCCACATCCATCCTGTAGGG
ATG5	CCGGGCAAGGTGGAGTTG	ACTCTTGGCAAAAGCAAATAGTATG
S6K1	GGGGGCTATGGAAAGGCAATG	ATCCACGATGAAGGGATGCTT
4E-BP1	CAAGGGATCTGCCCACCATT	AACTGTGACTCTTCACCGCC
RAPTOR	CCCCTACATGCCAGCTGAAC	CTTCCTGCCCCGTGTGATAG
RICTOR	TGGATCTGACCCGAGAACCT	ATATCGAAGCGCTCGTAGCC

detailed clinical parameters of RT-qPCR samples are summarized in Table S2. RNA quality and quantity were measured using the NanoDrop 1000 Spectrophotometer (Thermo Scientific, USA). cDNA was synthesized using the cDNA Synthesis SuperMix Kit. RT−qPCR was performed using a SYBR Green PCR kit with ABI StepOne instrument (Applied Biosystems, Foster City, CA, USA). Each 20 μl well reaction comprised of 10 μl of 2 × SYBR qPCR Mix, 1 μl of forward primer, 1 μl of reverse primer, 6 μl of RNase-free H2O and 2 μl of cDNA templates. Reactions were run under the following conditions: 95 °C for 10 min followed by 35 cycles of 15 s at 95 °C, 20 s at 60 °C and 15 s at 72 °C. For normalization, relative gene expression was calculated for each gene by the $2^{-\Delta\Delta CT}$ method with glyceraldehyde 3-phosphate dehydrogenase (GAPDH). The quantity and integrity of the RNA yield were assessed by using K5500 (Beijing Kaiao, China) and Agilent 2200 TapeStation (Agilent Technologies, USA), respectively. Briefly, total RNA was ligated with a 3′ RNA adapter, followed by 5′ adapter ligation. Subsequently, the adapter-ligated RNAs were subjected to RT–PCR and amplified with a low cycle. Then, the PCR products were size selected on a PAGE gel according to the NEBNext Multiplex Small RNA Library Prep Set for Illumina (Illumina, USA). Finally, the purified library products were evaluated using an Agilent 2200 TapeStation system and Qubit
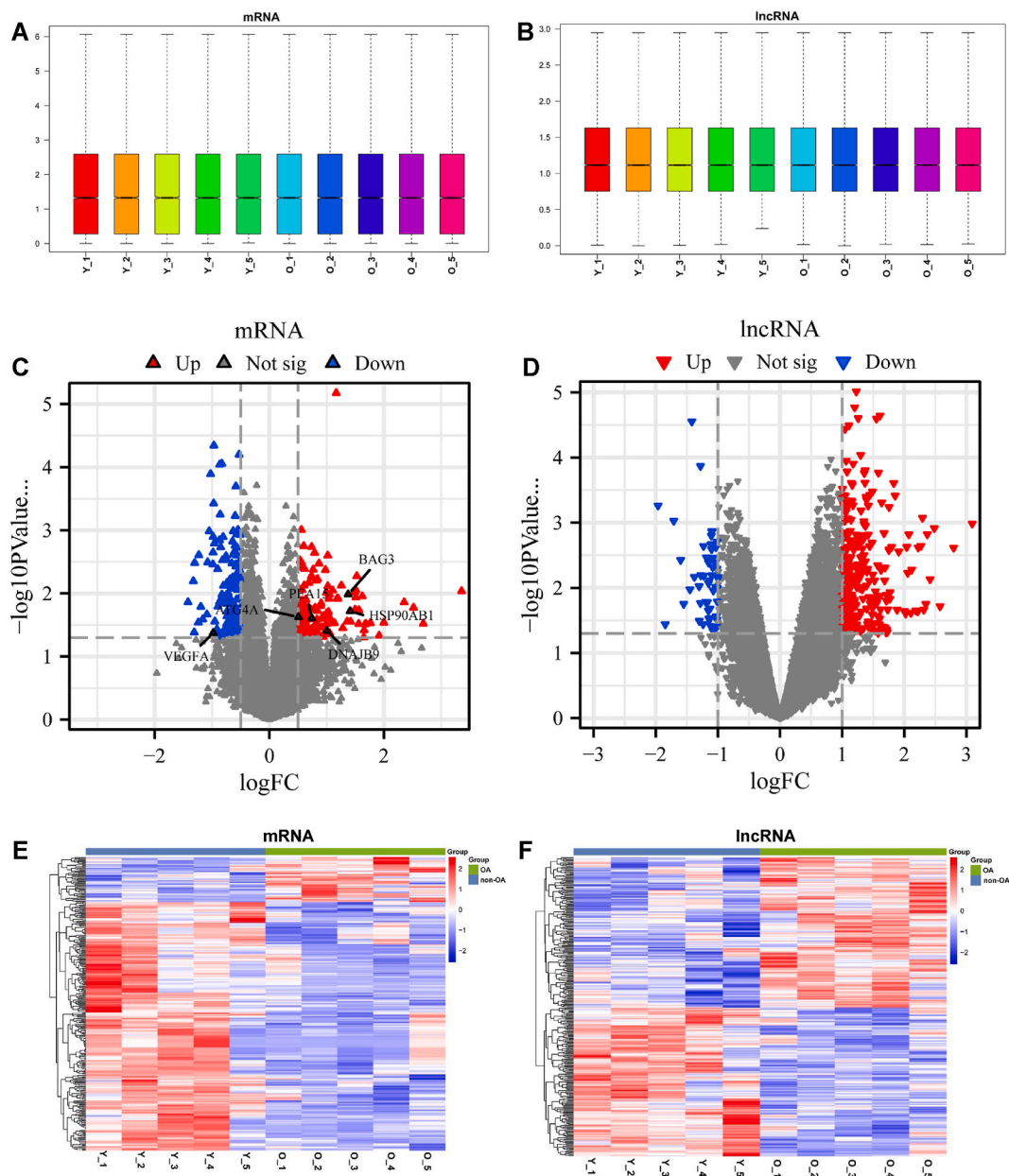

Fig. 1. Identification of DEMs and DELs. (A, B) The box plot of mRNA and lncRNA after normalization. (C, D) Volcano map of DEMs and DELs, the upregulated and downregulated genes are represented by red and blue, respectively. (E, F) Heatmap of DEMs and DELs. (For interpretation of the references to color in this figure legend, the reader is referred to the Web version of this article.)

(Thermo Fisher Scientific, USA). The libraries were sequenced on an Illumina HiSeq 2500 system (Illumina, USA) with a single-end 50 bp sequence at RiboBio Co., Ltd. The primer sequences for the genes used in this study are shown in Table 1.

4.5. Gene Set Enrichment Analysis (GSEA)

GSEA was employed to investigate the consistency and variability of phenotypes, aiming to identify common or distinct biological
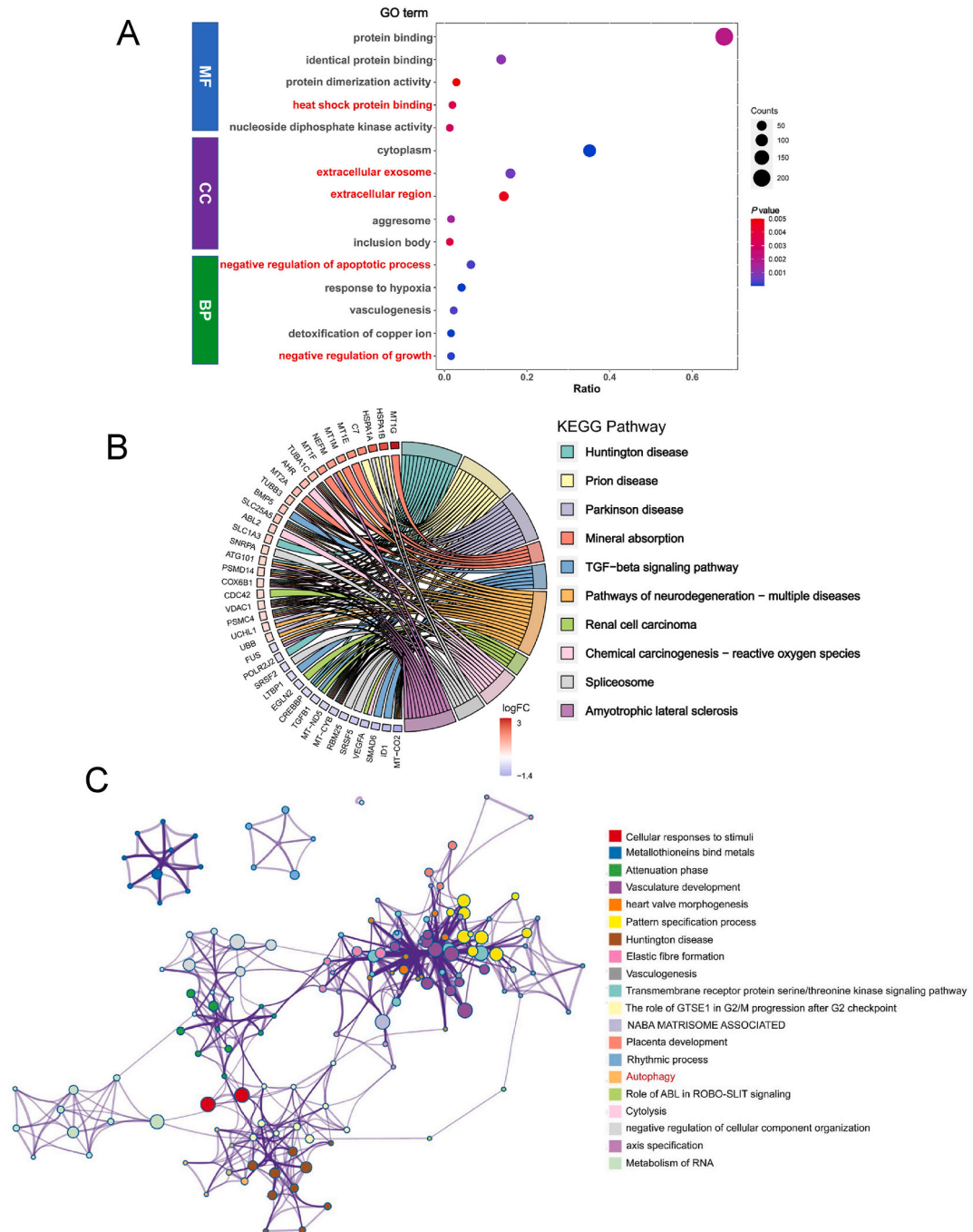

Fig. 2. Enrichment analysis of DEMs (A) Detailed variations information bubble diagrams of GO categories based on the DAVID database. (B) The chord plot shows the enrichment analysis results of DEMs and the top ten KEGG pathways based on the DAVID database, colors are represented by logFC values, red represents upregulated genes and blue represents downregulated genes (C) Network of enriched terms colored by cluster ID. (For interpretation of the references to color in this figure legend, the reader is referred to the Web version of this article.)

functions [25]. The samples were categorized into high and low expression group, based on the median expression levels of two hub genes: HSP90AB1 and BAG3. GSEA was performed using the "clusterprofiler" R package. The c2.cp.kegg.v6.0.symbols.gmt gene set, provided by the Molecular Signature Database (MSigDB), was utilized as the reference gene set. Following 10,000 permutations, enrichment pathways were identified based on *P* value < 0.05. The top 5 enriched pathways in both groups were visualized.

4.6. Statistical analysis

SPSS 20.0 (SPSS Science Inc., Chicago, Illinois, USA) and Prism 9.0 (GraphPad Software, La Jolla, CA, USA) were used to analyze experimental data. All data were expressed as mean ± standard error of the mean (S.E.M.). The significant differences in expression levels were tested using the student's two-tailed *t*-test as applicable. A value of $P < 0.05$ was considered statistically significant.

5. Result

5.1. Identification of DEMs and DELs

Upon converting the lncRNA and mRNA expression profiles into log2 values, boxplot visualizing the distribution of the normalized data were provided (Fig. 1A and B). The distribution of expression values across the samples remained consistent after normalization, suggesting the suitability of the data for subsequent analysis. By comparing the lncRNA and mRNA expression profiles between the OA meniscus group and non-OA meniscus group, we identified 320 DEMs, consisting of 161 upregulated DEMs and 159 downregulated DEMs. Additionally, we detected 310 DELs, comprising 260 upregulated DELs and 50 downregulated DELs. The volcano plots illustrating the DEMs and DELs are presented in Fig. 1C and D, respectively. Furthermore, heatmaps showcasing the expression patterns of the DEMs and DELs are shown in Fig. 1E and F, respectively.
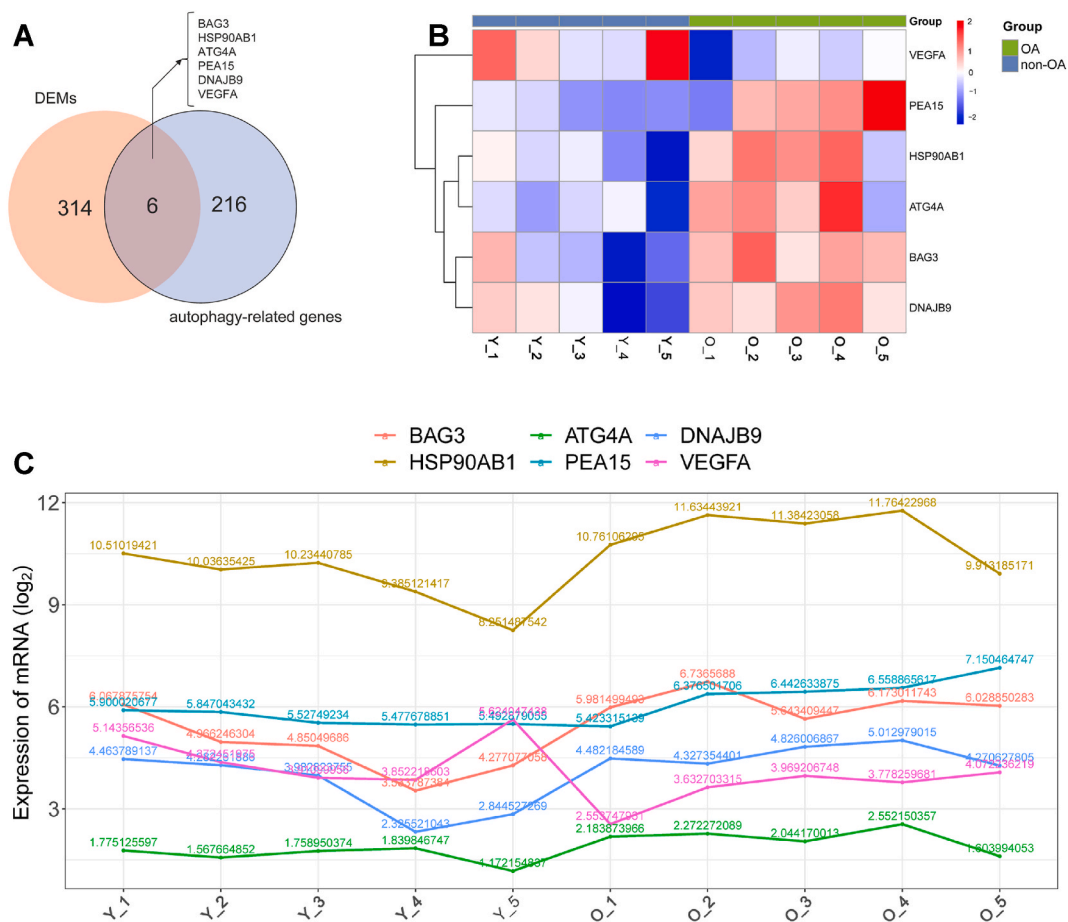

Fig. 3. Identification of autophagy-related DEMs. (A) Venn diagram of autophagy-related genes and DEMs. (B)The expression values of autophagy-related DEMs. (C) Heatmap of autophagy-related DEMs.

Fig. 4. lncRNA-miRNA-mRNA ceRNA network construction. (A) miRNA-mRNA network. Triangle represents miRNA, where red represents hub miRNA; Green circle represents mRNA. (B) Venn diagram of the predicted lncRNAs and DELs. (C) autophagy-related lncRNA-miRNA-mRNA network. ceRNA, competing endogenous RNA; DELs, differentially expressed lncRNAs. (For interpretation of the references to color in this figure legend, the reader is referred to the Web version of this article.)
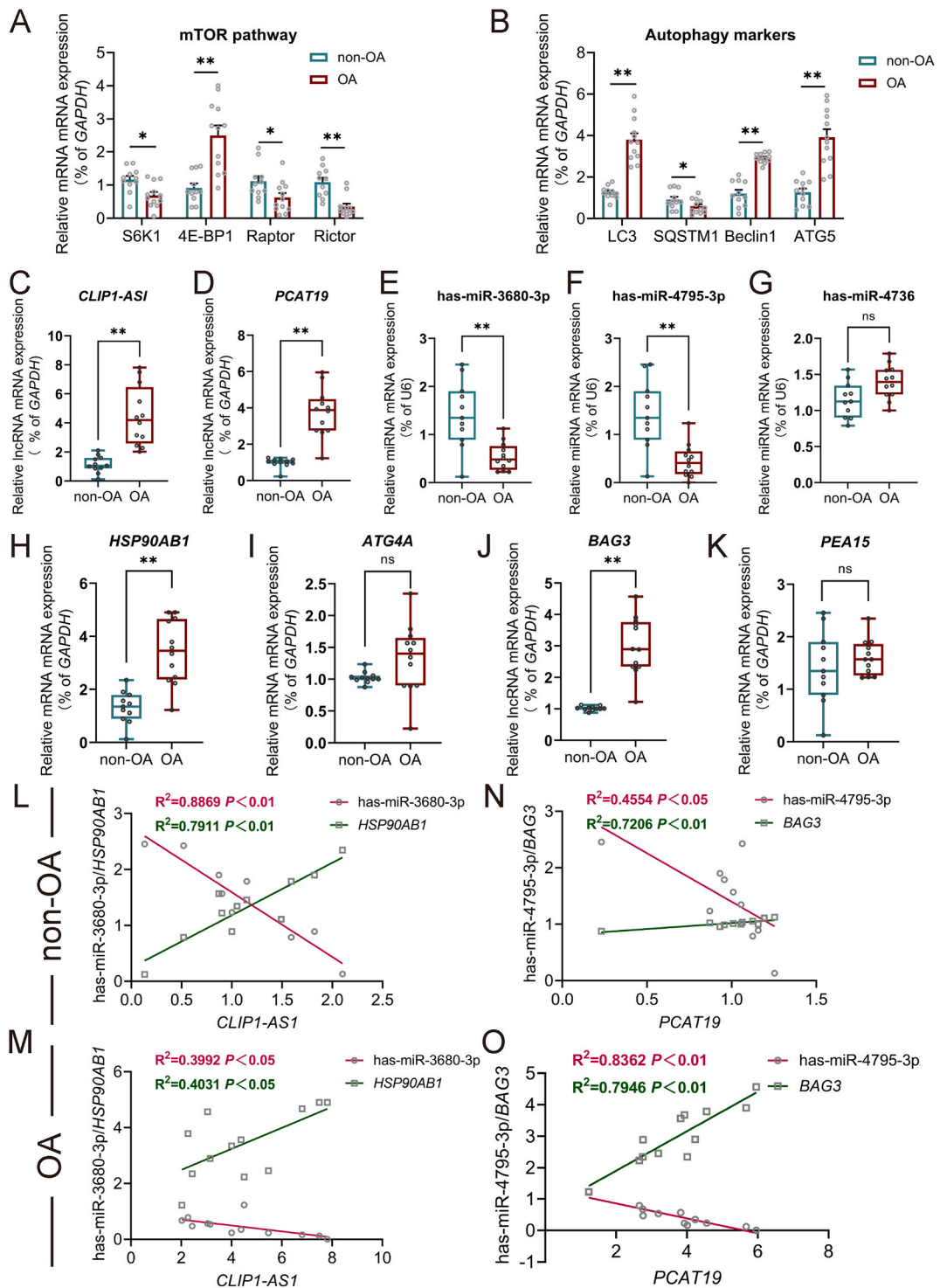
Fig. 5. RT-qPCR validation and correlation analysis. (A). RT-qPCR validation of mTOR signaling pathway related genes (S6K1, RAPTOR, RICTOR, and 4E-BP1). (B). RT-PCR validation of classical autophagy markers (LC3, Beclin1, ATG5, and SQSTM1). (C–K). RT-PCR validation of autophagy-related ceRNA network. (L–O) Correlation analysis between lncRNA, miRNA and mRNA. All experiments were performed in triplicate and results were presented as Mean ± S.E.D. (ns, no significance, $*P < 0.05$, $**P < 0.01$).

5.2. Enrichment analysis of DEMs and identification of autophagy-related DEMs

To gain further insights into the biological functions of these DEMs in meniscal degeneration, enrichment analyses were conducted. Utilizing the DAVID database, GO Molecular Function (GO-MF) analysis revealed that these DEMs were primarily enriched in nucleoside diphosphate kinase activity, heat shock protein binding, protein dimerization activity, identical protein binding, protein binding; GO Cell Component (GO-CC) analysis demonstrated their involvement in inclusion body, aggresome, extracellular region, extracellular exosome, cytoplasm; GO Biological Process (GO-BP) analysis revealed their associations with negative regulation of growth, detoxification of copper ion, vasculogenesis, response to hypoxia, negative regulation of apoptotic process (Fig. 2A). Additionally, KEGG enrichment analysis indicated that these DEMs were primarily associated with Huntington disease, prion disease, Parkinson disease, mineral absorption, TGF-beta signaling pathway, pathways of neurodegeneration-multiple diseases, renal cell carcinoma, chemical carcinogenesis-reactive oxygen species, spliceosome, amyotrophic lateral sclerosis, antigen processing and presentation, drug metabolism - other enzymes (Fig. 2B). All GO terms and KEGG pathways of DEMs are listed in Table S3. Furthermore, utilizing Metascape software, it was revealed that these DEMs were involved in autophagy-related pathways, as depicted in Fig. 2C. Previous studies have demonstrated that dysregulation of autophagic pathways could impact the integrity of intervertebral discs and cartilage, leading to impaired growth and degradation [26]. Moreover, autophagy has been extensively studied for its role in regulating apoptosis and was known to exert negative regulation on cell apoptosis [27] predominantly. These findings strongly suggested the involvement of these DEMs in autophagy-related pathways and their participation in the autophagy process. Consequently, by intersecting the 222 genes from the Human Autophagy Database with the 320 DEMs identified through the differential expression analysis, a set of six autophagy-related DEMs (BAG3, HSP90AB1, ATG4A, PEA15, DNAJB9 and VEGFA) were identified (Fig. 3A). The expression values of autophagy-related DEMs are presented in Fig. 3B and a heatmap visualizing their expression patterns is shown in Fig. 3C. All GO terms and KEGG pathways of autophagy-related DEMs are listed in Table S4.

5.3. Construction of lncRNA-miRNA-mRNA ceRNA network

To predict miRNAs targeting the autophagy-related DEMs, we conducted a comprehensive screening using TargetScan, miRmap, and miRDB databases. Specifically, we identified 19 miRNAs targeting HSP90AB1, 43 miRNAs targeting ATG4A, 26 miRNAs targeting BAG3, 104 miRNAs targeting DNAJB9, 6 miRNAs targeting VEGFA, and 100 miRNAs targeting PEA15 (Figs. S1A–F). Utilizing this information, we constructed and visualized a miRNA-mRNA network using Cytoscape (Fig. 4A). Since we did not find any miRNAs that could target all of the autophagy-related DEMs, we selected miRNAs that target more than 2 mRNAs, following previous reports [28]. As depicted in Fig. 3A, we identified 14 hub miRNAs for further analysis, namely hsa-miR-4795-3p, hsa-miR-126-5p, hsa-miR-4731-3p, hsa-miR-891b, hsa-miR-3680-3p, hsa-miR-561-3p, hsa-miR-4477b, hsa-miR-3671, hsa-miR-3064-5p, hsa--miR-6504-5p, hsa-miR-1277-5p, hsa-miR-3941, hsa-miR-1183, and hsa-miR-4736. Furthermore, we utilized the DIANA-LncBase Predicted database to predict potential lncRNAs targeting the aforementioned hub miRNAs. Through the intersection of the predicted lncRNAs and the differentially expressed lncRNAs, we identified three upregulated lncRNAs, namely CLIP1-AS1, PCBP1-AS1, and PCAT19 (Fig. 4B). Subsequently, by eliminating the miRNAs and mRNAs that did not exhibit an interaction relationship, we obtained ceRNA networks. These networks consisted of three upregulated hub lncRNAs (CLIP1-AS1, PCBP1-AS1, PCAT19), three miRNAs (has-miR-3680-3p, has-miR-4795-3p, has-miR-4736), and five upregulated mRNAs (ATG4A, PEA15, BAG3, HSP90AB1, DNAJB9) (Fig. 4C).

5.4. RT-qPCR verification and correlation analysis

The above KEGG enrichment analysis of autophagy-related DEMs revealed the involvement of PI3K-ATK signaling Pathway. Increasing evidence reported the involvement of the PI3K/AKT/mTOR pathway in the development of OA [29]. Moreover, the mTOR pathway served as a critical autophagy inhibitor and was regulated by the upstream PI3K/ATK signaling pathway [30]. Therefore, we analyzed the mRNA expression levels of mTOR pathway-related markers (S6K1, 4E-BP1, RAPTOR, and RICTOR) [31–33]. The results showed that the expression values of S6K1, RAPTOR, and RICTOR were lower in the OA group compared to the non-OA group, while 4E-BP1 showed higher expression in the OA group. These results indicated that the mTOR signaling pathway in the OA meniscus was suppressed.

In assessing the autophagy expression levels in the OA meniscus, the classical autophagy markers (LC3, Beclin1, ATG5, and SQSTM1) [34–36], were evalated. The findings revealed that the expression levels of LC3, Beclin1, and ATG5 showed a significant increase, while the expression of SQSTM1 was decreased in the OA meniscus group compared to the non-OA meniscus group (Fig. 5B). These results indicated that the autophagy level in the OA meniscus group was notably higher than that in the non-OA meniscus group.

In addition, to validate the expression levels of three lncRNAs (CLIP1-AS1, PCBP1-AS1, PCAT19), three miRNA (has-miR-3680-3p, has-miR-4795-3p, has-miR-4736) and five mRNAs (ATG4A, PEA15, BAG3, HSP90AB1, DNAJB9) in the autophagy-related ceRNA network mentioned above, RT-qPCR was performed. However, due to unsatisfactory PCR amplification results after multiple pretests, PCBP1-AS1 and DNAJB9 were automatically excluded from further analysis. Our findings revealed that the expression values of CLIP1-AS1 ($P < 0.01$, Fig. 5C), PCAT19 ($P < 0.01$, Fig. 5D), HSP90AB1 ($P < 0.01$, Fig. 5H), and BAG3 ($P < 0.01$, Fig. 5J) were significantly higher, and the expression values of has-miR-3680-3p ($P < 0.01$, Fig. 5E) and has-miR-4795-3p ($P < 0.01$, Fig. 5F) were significantly reduced in the OA meniscus group compared to the non-OA meniscus group. However, no significant differences were observed in the expression levels of has-miR-4736, ATG4A and PEA15 between the two groups (Fig. 5G–I, K). Meanwhile, in order to investigate potential regulatory mechanisms, we performed correlation analysis between lncRNA, miRNA, and mRNA. Our results indicated a

strong positive correlation between CLIP1-AS1 and HSP90AB1, as well as between PCAT19 and BAG3 (Fig. 5L-O). Conversely, a strong negative correlation was observed between CLIP1-AS1 and miR-3680-3p, as well as between PCAT19 and miR-4795-3p (Fig. 5L–O), both in the non-OA meniscus and OA meniscus groups. These results aligned with the RNA sequencing analysis, thus confirming the elevated expression levels of CLIP1-AS1, PCAT19, HSP90AB1, and BAG3 in the OA meniscus group.

5.5. Gene set enrichment analysis of HSP90AB1 and BAG3

To gain further insights into the potential biological pathways associated with meniscal degeneration and the autophagy-related mRNAs HSP90AB1 and BAG3, we conducted GSEA using a single-gene approach, following previously established methods [37]. For HSP90AB1, the results revealed significant activation (normalized enrichment score [NES] > 0) in the citrate cycle, legionellosis, mineral absorption, protein export, and steroid biosynthesis pathways (Fig. 6A). Conversely, the adipocytokine signaling pathway, glycosaminoglycan biosynthesis−chondroitin sulfate, glycosaminoglycan biosynthesis−heparan sulfate, glycosaminoglycan biosynthesis−keratan sulfate, mannose type O−glycan biosynthesis were significantly inactivated (NES <0) concerning HSP90AB1 (Fig. 6B). Regarding BAG3, the GSEA results indicated significant activation (NES >0) in the legionellosis, longevity regulating pathway, metabolism of xenobiotics by cytochrome P450, mineral absorption and proximal tubule bicarbonate reclamation (Fig. 6C). In contrast, asthma, ECM−receptor interaction, glycosaminoglycan biosynthesis−chondroitin sulfate, glycosaminoglycan biosynthesis−heparan sulfate, protein digestion and absorption were significantly inactivated (NES <0) about BAG3 (Fig. 6D). Based on these findings, it could be inferred that both HSP90AB1 and BAG3 might inhibit the glycosaminoglycan biosynthesis.
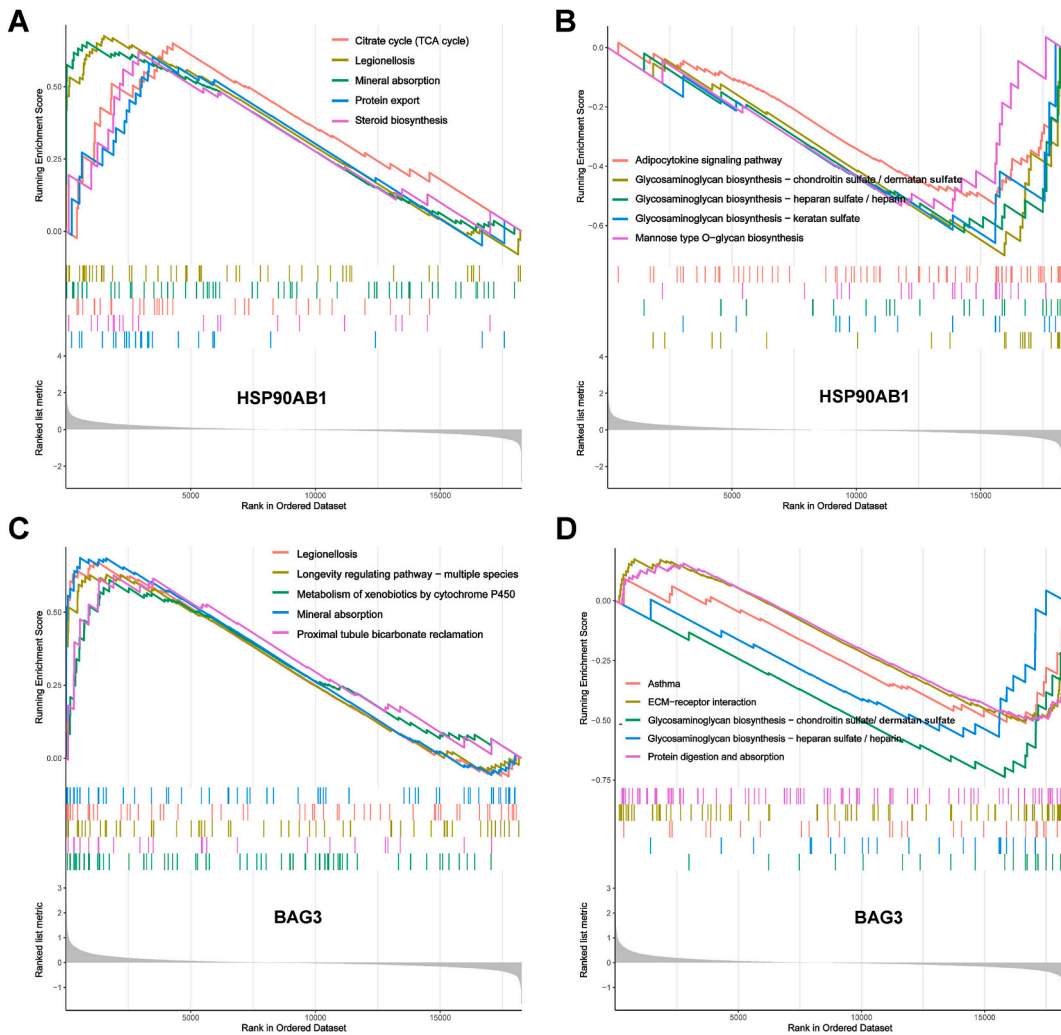

Fig. 6. Gene set enrichment analysis of autophagy-related mRNAs. (A, B) Gene set enrichment analysis (GSEA) pathways enriched by HSP90AB1. (C, D) Gene set enrichment analysis (GSEA) pathways enriched by BAG3.

6. Discussion

The aging process leads to a loss of elasticity in the meniscus, resulting in increased stiffness and impaired function, ultimately leading to degeneration of the meniscus and cartilage [38]. Various factors such as age, body mass index (BMI), gender, genetic predisposition, and intra-articular injury have been recognized as contributors to meniscal and cartilage degeneration [39]. According to an early study conducted by Sun et al., it was discovered that meniscal cells might actively contribute to the development of OA [40]. Consequently, it becomes crucial to impede the progression of meniscal degeneration as individuals age, as this can aid in preventing meniscal injuries and OA in middle-aged and elderly patients. However, the precise regulatory mechanism underlying meniscus degeneration remains unclear. With the growing understanding of the influence of genomic and epigenetic changes on disease processes, investigating the regulatory mechanisms associated with meniscus degeneration has become increasingly feasible and essential. Numerous studies have demonstrated that autophagy activation could attenuate chondrocyte cell death in the early stages of OA. In a recent study by Liao et al., it was reported that HECTD1-mediated Rubicon regulates chondrocyte autophagy, leading to a reduction in chondrocyte death and subsequently slowing the progression of OA [41]. However, it is important to note that excessive activation of autophagy may induce chondrocyte cell death [42]. Therefore, further research is warranted to elucidate the precise role of autophagy in cartilage. LncRNA has emerged as a key player in cartilage development, with abnormal expression contributing to cartilage degradation in OA [43]. In a study conducted by Ai LY et al., they investigated the regulatory relationships between lncRNAs and mRNAs that may contribute to the changes observed in aged meniscus. Through analysis of lncRNA and mRNA expression profiles, they identified several significant associations. Specifically, they found that AP001011 inhibited the expression of TNFRSF11B, while AC1243125 upregulated its expression. Additionally, POC1B-AS1 was shown to regulate BMP2 expression by acting as a sponge for miR-130a-3p, miR-136-5p, miR-18a-3p, and miR-60 [44]. Furthermore, the crucial role of lncRNA as a regulatory factor in autophagy and apoptosis in chondrocytes has recently gained recognition [45]. However, the involvement of autophagy-related lncRNAs in meniscal degeneration associated with osteoarthritis has not been explored. Consequently, the objective of this study was to identify autophagy-related lncRNAs and elucidate their regulatory mechanisms in the context of osteoarthritis-related meniscal degeneration through a combination of bioinformatics analysis and in vitro validation.

In this study, we conducted RNA sequencing analysis on human meniscus samples, identifying 310 DELs and 320 DEMs. We compared DEMs and DELs with several other datasets (GSE191157, GSE52042 and GSE19060) based on RNA-seq in meniscal and found that the shared DEMs and DELs among these datasets were not completely consistent [40,44,46]. We assumed that the inconsistencies among the different datasets were not only due to the differences in race, age, sex, and tissue sites [47], but also owing to the batch effect of sequencing and different platforms utilized in the respective research [48]. Utilizing bioinformatics functional analysis based on the DAVID database, GO term analysis revealed that these DEMs were primarily associated with the extracellular region, extracellular exosome, negative regulation of growth, heat shock protein binding, response to hypoxia and negative regulation of apoptotic process. The progressive deterioration of the meniscus structure in meniscal degeneration directly impacted its functionality [49,50]. Furthermore, the KEGG pathway enrichment analysis demonstrated that these DEMs were prominently involved in Huntington disease, prion disease, Parkinson disease, mineral absorption, TGF-beta signaling pathway, pathways of neurodegeneration-multiple diseases, renal cell carcinoma, chemical carcinogenesis-reactive oxygen species, spliceosome, amyotrophic lateral sclerosis, antigen processing and presentation and drug metabolism-other enzymes. It has been well-established that the pathogenesis of neurodegeneration-multiple diseases, Parkinson disease, and Huntington disease were closely linked to autophagy and aging [51]. Moreover, the TGF-beta signaling pathway played a crucial role in regulating autophagy in articular cartilage and maintaining the stability of articular chondrocytes [52]. Further analysis using Metascape confirmed the association of these DEMs with autophagy. Based on the intersection of the DEMs from RNA sequencing and autophagy-related mRNAs obtained from HADb, we identified six differentially expressed autophagy-related mRNAs in the OA meniscus. In our study, we observed enrichment of autophagy-related DEMs within the PI3K-AKT signaling pathway. It is well-established that PI3K/Akt signaling pathway was the upstream of mTOR signaling pathway, while mTOR pathway served as a critical autophagy inhibitor [29], implying the potential involvement of the mTOR signaling pathway in the regulation of autophagy in the meniscus. Furthermore, our RT-qPCR results demonstrated suppressed activity of the mTOR signaling pathway in the meniscus affected by OA, which coincided with an observed increase in autophagy levels. Subsequently, we constructed autophagy-related lncRNA-miRNA-mRNA regulatory networks. The DELs and DEMs were further validated using RT-qPCR, leading to the identification of two autophagy-related lncRNA-miRNA-mRNA regulatory networks: CLIP1-AS1/has-miR-3680-3p/HSP90AB1 and PCAT19/has-miR-4795-3p/BAG3.

Within the autophagy-related ceRNA networks, we identified two downstream autophagy-related mRNAs: BAG3 and HSP90AB1. BAG3, a unique member of the co-chaperone family, interacts with other binding partners and has been demonstrated to participate in apoptosis and autophagy [53]. A study by Lu et al. revealed a significant increase in BAG3 expression and its involvement in autophagy regulation in chondrocytes of lumbar facet joint osteoarthritis [53]. HSP90AB1, a member of the heat shock protein family A (HSP90), is a molecular chaperone and plays crucial roles in protein folding and quality control [54]. Inhibition of Hsp90 has been shown to impede tau protein clearance, leading to the accumulation of neurotoxic tau and an increased risk of neurodegenerative diseases [55]. However, before our study, no reports have linked BAG3 and HSP90AB1 to meniscal degeneration. Meniscal cells are fibrochondrocytes comprising a dense extracellular matrix (ECM) consisting of water, primarily type II collagen, glycosaminoglycans (GAGs), and proteoglycans [56]. GAGs play a vital role in maintaining the viscoelastic properties and overall function of the meniscus and cartilage, enhancing their ability to resist loading and pressure [56,57]. Furthermore, the degree of GAG depletion is directly associated with decreased resistance to shear deformation [58]. Through GSEA, we observed that elevated expression of BAG3 and HSP90AB1 could inhibit the biosynthesis of GAGs and the synthesis of the extracellular matrix. Therefore, we speculated that high expression of autophagy-related mRNAs (HSP90AB1 and BAG3) could impact the ECM integrity of meniscal cells by suppressing the

anabolic metabolism of GAG, leading to the reduced ability of resistance to shear deformation and further causing meniscal degeneration in OA meniscus.

Several studies have demonstrated the involvement of lncRNAs in regulating the dynamic processes of autophagy [59,60]. Within the autophagy-related lncRNA-mRNA-miRNA competing endogenous RNA networks, we identified two upstream autophagy-related lncRNAs: PCAT19 and CLIP1-AS1. In addition, we found that CLIP1-AS1/HSP90AB1 and PCAT19/BAG3 both have a strong positive correlation, while miR-3680-3p/CLIP1-AS1 and miR-4795-3p/PCAT19 have a strong negative correlation. Specifically, PCAT19 was predicted to function as a ceRNA by sequestering hsa-miR-4795-3p, thereby regulating the expression of BAG3. Previous research has shown that upregulation of PCAT19 inhibited cell proliferation by modulating the miR-25-3p/MAP2k4 signaling axis and promoted cell apoptosis in lung cancer [61]. Moreover, PCAT19 overexpression enhanced the expression of Follistatin-Related Protein 1 (FSTL1), subsequently activating autophagy and impacting airway remodeling and inflammatory phenotypes [62]. Although PCAT19 has been implicated in autophagy regulation in other diseases, its role in meniscal degeneration in OA has not been previously reported. Based on GSEA and correlation analysis, we speculated that PCAT9 is involved in the inhibition of GAG anabolic metabolism in the OA meniscus by regulating BAG3 expression via competitive targeting of miR-4795-3p. Additionally, our findings indicated that CLIP1-AS1 could act as a ceRNA, sequestering has-miR-3680-3p and thereby modulating the expression of HSP90AB1. However, the specific role of CLIP1-AS1 in meniscal degeneration in OA remains unclear. Similarly, considering the results obtained from GSEA and correlation analysis, we postulated that the inhibition of GAG anabolic metabolism in the OA meniscus might be associated with the upregulation of HSP90AB1 promoted by CLIP1-AS1 vis competitive targeting of miR-4795-3p. Overall, identifying these two autophagy-related lncRNAs in the OA meniscus, potentially hindering GAG anabolic metabolism, provided crucial insights into the underlying mechanisms of meniscal degeneration and identified novel therapeutic targets.

However, our study has some limitations. Firstly, due to data availability constraints, miRNAs were predicted using public databases. Further experimental investigations are necessary to fully comprehend the regulatory network and explore their biological significance in cellular or animal models.

7. Conclusion

In this study, for the first time, we identified two autophagy-related ceRNA networks based on our RNA sequencing and in vitro validation, which contained two lncRNAs (CLIP1-AS1, PCAT19), two miRNAs (has-miR-3680-3p, has-miR-4795-3p) and two mRNA (BAG3, HSP90AB1). These new insights will deepen our understanding of meniscal degeneration and may provide important clues for therapeutic strategies.

Ethics approval and consent to participate

Our study was approved by the Ethics Committee of Zhongnan Hospital of Wuhan University (No.2022069K).

Consent for publication

Not applicable.

Data availability statement

The datasets used and/or analyzed during the current study are available from the corresponding author on reasonable request. The names of the repository/repositories and accession number(s) can be found below: GEO, GSE263210.

CRediT authorship contribution statement

Jun Zhang: Writing – original draft, Methodology, Investigation, Data curation. **Jiayong Zhu:** Validation, Methodology. **Xinyu Zou:** Visualization, Methodology. **Yiming Liu:** Data curation. **Boming Zhao:** Visualization, Data curation. **Liaobin Chen:** Writing – review & editing, Funding acquisition. **Bin Li:** Writing – review & editing, Supervision, Conceptualization. **Biao Chen:** Writing – review & editing, Supervision, Conceptualization.

Declaration of competing interest

The authors declare that they have no known competing financial interests or personal relationships that could have appeared to influence the work reported in this paper.

Acknowledgements

Appendix A. Supplementary data

Supplementary data to this article can be found online at https://doi.org/10.1016/j.heliyon.2024.e32782.

References

[1] P. Renström, R.J. Johnson, Anatomy and biomechanics of the menisci, Clin. Sports Med. 9 (3) (1990) 523–538.

[2] M. Englund, F.W. Roemer, D. Hayashi, M.D. Crema, A. Guermazi, Meniscus pathology, osteoarthritis and the treatment controversy, Nat. Rev. Rheumatol. 8 (7) (2012) 412–419.

[3] M. Englund, A. Guermazi, D. Gale, D.J. Hunter, P. Aliabadi, M. Clancy, et al., Incidental meniscal findings on knee MRI in middle-aged and elderly persons, N. Engl. J. Med. 359 (11) (2008) 1108–1115.

[4] S. Jung, H. Jeong, S.W. Yu, Autophagy as a decisive process for cell death, Exp. Mol. Med. 52 (6) (2020) 921–930.

[5] B. Levine, G. Kroemer, Autophagy in the pathogenesis of disease, Cell 132 (1) (2008) 27–42.

[6] G. Musumeci, P. Castrogiovanni, F.M. Trovato, A.M. Weinberg, M.K. Al-Wasiyah, M.H. Alqahtani, et al., Biomarkers of chondrocyte apoptosis and autophagy in osteoarthritis, Int. J. Mol. Sci. 16 (9) (2015) 20560–20575.

[7] T.W. Zhang, Z.F. Li, J. Dong, L.B. Jiang, The circadian rhythm in intervertebral disc degeneration: an autophagy connection, Exp. Mol. Med. 52 (1) (2020) 31–40.

[8] J.K. Meckes, B. Caramés, M. Olmer, W.B. Kiosses, S.P. Grogan, M.K. Lotz, et al., Compromised autophagy precedes meniscus degeneration and cartilage damage in mice, Osteoarthritis Cartilage 25 (11) (2017) 1880–1889.

[9] L. Salmena, L. Poliseno, Y. Tay, L. Kats, P.P. Pandolfi, A ceRNA hypothesis: the Rosetta Stone of a hidden RNA language? Cell 146 (3) (2011) 353–358.

[10] L. Statello, C.J. Guo, L.L. Chen, M. Huarte, Gene regulation by long non-coding RNAs and its biological functions, Nat. Rev. Mol. Cell Biol. 22 (2) (2021) 96–118.

[11] J. Zhu, W. Yu, Y. Wang, K. Xia, Y. Huang, A. Xu, et al., lncRNAs: function and mechanism in cartilage development, degeneration, and regeneration, Stem Cell Res. Ther. 10 (1) (2019) 344.

[12] M.J. Pearson, A.M. Philp, J.A. Heward, B.T. Roux, D.A. Walsh, E.T. Davis, et al., Long Intergenic noncoding RNAs mediate the human chondrocyte inflammatory response and are differentially expressed in osteoarthritis cartilage, Arthritis Rheumatol. 68 (4) (2016) 845–856.

[13] M. Krawczyk, B.M. Emerson, p50-associated COX-2 extragenic RNA (PACER) activates COX-2 gene expression by occluding repressive NF-κB complexes, Elife 3 (2014) e01776.

[14] Z. Che, J. Xueqin, Z. Zhang, LncRNA OIP5-AS1 accelerates intervertebral disc degeneration by targeting miR-25-3p, Bioengineered 12 (2) (2021) 11201–11212.

[15] C.L. Wang, J.P. Peng, X.D. Chen, LncRNA-CIR promotes articular cartilage degeneration in osteoarthritis by regulating autophagy, Biochem. Biophys. Res. Commun. 505 (3) (2018) 692–698.

[16] Z. Sun, X. Tang, H. Wang, H. Sun, P. Chu, L. Sun, et al., LncRNA H19 aggravates intervertebral disc degeneration by promoting the autophagy and apoptosis of nucleus pulposus cells through the miR-139/CXCR4/NF-κB Axis, Stem Cell. Dev. 30 (14) (2021) 736–748.

[17] A. Mortazavi, B.A. Williams, K. McCue, L. Schaeffer, B. Wold, Mapping and quantifying mammalian transcriptomes by RNA-Seq, Nat. Methods 5 (7) (2008) 621–628.

[18] W. Huang da, B.T. Sherman, R.A. Lempicki, Systematic and integrative analysis of large gene lists using DAVID bioinformatics resources, Nat. Protoc. 4 (1) (2009) 44–57.

[19] Y. Zhou, B. Zhou, L. Pache, M. Chang, A.H. Khodabakhshi, O. Tanaseichuk, et al., Metascape provides a biologist-oriented resource for the analysis of systems-level datasets, Nat. Commun. 10 (1) (2019) 1523.

[20] D. Bu, H. Luo, P. Huo, Z. Wang, S. Zhang, Z. He, et al., KOBAS-i: intelligent prioritization and exploratory visualization of biological functions for gene enrichment analysis, Nucleic Acids Res. 49 (W1) (2021) W317, w25.

[21] S.E. McGeary, K.S. Lin, C.Y. Shi, T.M. Pham, N. Bisaria, G.M. Kelley, et al., The biochemical basis of microRNA targeting efficacy, Science (New York, NY) 366 (6472) (2019).

[22] C.E. Vejnar, E.M. Zdobnov, MiRmap: comprehensive prediction of microRNA target repression strength, Nucleic Acids Res. 40 (22) (2012) 11673–11683.

[23] Y. Chen, X. Wang, miRDB: an online database for prediction of functional microRNA targets, Nucleic Acids Res. 48 (D1) (2020) D127, d31.

[24] M.D. Paraskevopoulou, I.S. Vlachos, D. Karagkouni, G. Georgakilas, I. Kanellos, T. Vergoulis, et al., DIANA-LncBase v2: indexing microRNA targets on non-coding transcripts, Nucleic Acids Res. 44 (D1) (2016) D231–D238.

[25] A. Subramanian, P. Tamayo, V.K. Mootha, S. Mukherjee, B.L. Ebert, M.A. Gillette, et al., Gene set enrichment analysis: a knowledge-based approach for interpreting genome-wide expression profiles, Proc. Natl. Acad. Sci. U.S.A. 102 (43) (2005) 15545–15550.

[26] V. Madhu, A.R. Guntur, M.V. Risbud, Role of autophagy in intervertebral disc and cartilage function: implications in health and disease, Matrix Biol. : journal of the International Society for Matrix Biology 100–101 (2021) 207–220.

[27] D.R. Miller, S.D. Cramer, A. Thorburn, The interplay of autophagy and non-apoptotic cell death pathways, International review of cell and molecular biology 352 (2020) 159–187.

[28] H. Zhang, C. Bian, S. Tu, F. Yin, P. Guo, J. Zhang, et al., Integrated analysis of lncRNA-miRNA-mRNA ceRNA network in human aortic dissection, BMC Genom. 22 (1) (2021) 724.

[29] K. Sun, J. Luo, J. Guo, X. Yao, X. Jing, F. Guo, The PI3K/AKT/mTOR signaling pathway in osteoarthritis: a narrative review, Osteoarthritis Cartilage 28 (4) (2020) 400–409.

[30] C.C. Dibble, L.C. Cantley, Regulation of mTORC1 by PI3K signaling, Trends Cell Biol. 25 (9) (2015) 545–555.

[31] W.J. Oh, E. Jacinto, mTOR complex 2 signaling and functions, Cell Cycle 10 (14) (2011) 2305–2316.

[32] K. Hara, Y. Maruki, X. Long, K. Yoshino, N. Oshiro, S. Hidayat, et al., Raptor, a binding partner of target of rapamycin (TOR), mediates TOR action, Cell 110 (2) (2002) 177–189.

[33] D.C. Fingar, C.J. Richardson, A.R. Tee, L. Cheatham, C. Tsou, J. Blenis, mTOR controls cell cycle progression through its cell growth effectors S6K1 and 4E-BP1/eukaryotic translation initiation factor 4E, Mol. Cell Biol. 24 (1) (2004) 200–216.

[34] L. Don Wai Luu, N.O. Kaakoush, N. Castaño-Rodríguez, The role of ATG16L2 in autophagy and disease, Autophagy 18 (11) (2022) 2537–2546.

[35] A.V. Kumar, J. Mills, L.R. Lapierre, Selective autophagy receptor p62/SQSTM1, a pivotal player in stress and aging, Front. Cell Dev. Biol. 10 (2022) 793328.

[36] Y. Wei, S. Pattingre, S. Sinha, M. Bassik, B. Levine, JNK1-mediated phosphorylation of Bcl-2 regulates starvation-induced autophagy, Mol. Cell 30 (6) (2008) 678–688.

[37] Q. Dong, Z. Han, L. Tian, Identification of serum exosome-derived circRNA-miRNA-TF-mRNA regulatory network in postmenopausal Osteoporosis using bioinformatics analysis and validation in Peripheral blood-derived mononuclear cells, Front. Endocrinol. 13 (2022) 899503.

[38] M.A. Wesdorp, S.M. Eijgenraam, D.E. Meuffels, S.M.A. Bierma-Zeinstra, G.J. Kleinrensink, Y.M. Bastiaansen-Jenniskens, et al., Traumatic meniscal tears are associated with meniscal degeneration, Am. J. Sports Med. 48 (10) (2020) 2345–2352.

[39] J.N. Katz, K.R. Arant, R.F. Loeser, Diagnosis and treatment of hip and knee osteoarthritis: a review, JAMA 325 (6) (2021) 568–578.

[40] Y. Sun, D.R. Mauerhan, P.R. Honeycutt, J.S. Kneisl, J.H. Norton, E.N. Hanley Jr., et al., Analysis of meniscal degeneration and meniscal gene expression, BMC Muscoskel. Disord. 11 (2010) 19.

[41] S. Liao, Q. Zheng, H. Shen, G. Yang, Y. Xu, X. Zhang, et al., HECTD1-Mediated ubiquitination and degradation of Rubicon regulates autophagy and osteoarthritis pathogenesis, Arthritis Rheumatol. 75 (3) (2023) 387–400.

[42] R. Duan, H. Xie, Z.Z. Liu, The role of autophagy in osteoarthritis, Front. Cell Dev. Biol. 8 (2020) 608388.

[43] J. Wang, Y. Sun, J. Liu, B. Yang, T. Wang, Z. Zhang, et al., Roles of long non-coding RNA in osteoarthritis, Int. J. Mol. Med. 48 (1) (2021) (Review).

[44] L.-Y. Ai, M.-Z. Du, Y.-R. Chen, P.-Y. Xia, J.-Y. Zhang, D. Jiang, Integrated analysis of lncRNA and mRNA expression profiles indicates age-related changes in meniscus, Front. Cell Dev. Biol. 10 (2022).

[45] S. Jiang, Y. Liu, B. Xu, Y. Zhang, M. Yang, Noncoding RNAs: new regulatory code in chondrocyte apoptosis and autophagy, Wiley interdisciplinary reviews RNA 11 (4) (2020) e1584.

[46] H. Muhammad, B. Schminke, C. Bode, M. Roth, J. Albert, S. von der Heyde, et al., Human migratory meniscus progenitor cells are controlled via the TGF-β pathway, Stem Cell Rep. 3 (5) (2014) 789–803.

[47] Y.M. Golightly, J.B. Renner, C.G. Helmick, J.M. Jordan, A.E. Nelson, Looking back on 30+ years of the johnston county osteoarthritis project while looking forward with the Johnston County health study: a narrative review, Osteoarthritis Cartilage 32 (4) (2024) 430–438.

[48] J.T. Leek, W.E. Johnson, H.S. Parker, A.E. Jaffe, J.D. Storey, The sva package for removing batch effects and other unwanted variation in high-throughput experiments, Bioinformatics 28 (6) (2012) 882–883.

[49] M.P. Hellio Le Graverand, E. Vignon, I.G. Otterness, D.A. Hart, Early changes in lapine menisci during osteoarthritis development: Part I: cellular and matrix alterations, Osteoarthritis Cartilage 9 (1) (2001) 56–64.

[50] J. Kwok, S. Grogan, B. Meckes, F. Arce, R. Lal, D. D'Lima, Atomic force microscopy reveals age-dependent changes in nanomechanical properties of the extracellular matrix of native human menisci: implications for joint degeneration and osteoarthritis, Nanomed. Nanotechnol. Biol. Med. 10 (8) (2014) 1777–1785.

[51] M. Tran, P.H. Reddy, Defective autophagy and mitophagy in aging and Alzheimer's disease, Front. Neurosci. 14 (2020) 612757.

[52] C. Wang, J. Shen, J. Ying, D. Xiao, R.J. O'Keefe, FoxO1 is a crucial mediator of TGF-β/TAK1 signaling and protects against osteoarthritis by maintaining articular cartilage homeostasis, Proc. Natl. Acad. Sci. U.S.A. 117 (48) (2020) 30488–30497.

[53] X. Lu, J. Zhang, P. Xue, Q. Wang, X. Wang, Y. Sun, et al., BAG3 protects chondrocytes against lumbar facet joint osteoarthritis by regulating autophagy and apoptosis, J. Physiol. Biochem. 78 (2) (2022) 427–437.

[54] L.H. Pearl, C. Prodromou, Structure and mechanism of the Hsp90 molecular chaperone machinery, Annu. Rev. Biochem. 75 (2006) 271–294.

[55] L.J. Blair, B.A. Nordhues, S.E. Hill, K.M. Scaglione, J.C. O'Leary 3rd, S.N. Fontaine, et al., Accelerated neurodegeneration through chaperone-mediated oligomerization of tau, J. Clin. Invest. 123 (10) (2013) 4158–4169.

[56] A.J. Fox, A. Bedi, S.A. Rodeo, The basic science of human knee menisci: structure, composition, and function, Sports health 4 (4) (2012) 340–351.

[57] J. Sanchez-Adams, V.P. Willard, K.A. Athanasiou, Regional variation in the mechanical role of knee meniscus glycosaminoglycans, J. Appl. Physiol. 111 (6) (2011) 1590–1596.

[58] G. Han, U. Boz, M. Eriten, C.R. Henak, Glycosaminoglycan depletion increases energy dissipation in articular cartilage under high-frequency loading, J. Mech. Behav. Biomed. Mater. 110 (2020) 103876.

[59] H. Yao, B. Han, Y. Zhang, L. Shen, R. Huang, Non-coding RNAs and autophagy, Adv. Exp. Med. Biol. 1206 (2019) 199–220.

[60] Q. Ma, S. Long, Z. Gan, G. Tettamanti, K. Li, L. Tian, Transcriptional and post-transcriptional regulation of autophagy, Cells 11 (3) (2022).

[61] B. Wang, S. Yang, Y. Jia, J. Yang, K. Du, Y. Luo, et al., PCAT19 regulates the proliferation and apoptosis of lung cancer cells by inhibiting miR-25-3p via targeting the MAP2K4 signal Axis, Dis. Markers 2022 (2022) 2442094.

[62] F. Liu, J. Zhang, D. Zhang, Q. Qi, W. Cui, Y. Pan, et al., Follistatin-related protein 1 in asthma: miR-200b-3p interactions affect airway remodeling and inflammation phenotype, Int. Immunopharm. 109 (2022) 108793.